ELSEVIER

Journal of Power Sources 97–98 (2001) 688–692

JOURNAL OF POWER SOURCES

www.elsevier.com/locate/jpowsour

Comparative study of thermal behaviors of various lithium-ion cells

Yoshiyasu Saito*, Kiyonami Takano, Katsuhiko Kanari, Akira Negishi, Ken Nozaki, Ken Kato

Electrotechnical Laboratory, 1-1-4 Umezono, Tsukuba, Ibaraki 305-8568, Japan

Received 20 June 2000; accepted 7 January 2001

Abstract

Heat generation behaviors during charge and discharge are examined by calorimetric measurement for several lithium-ion cells that are commercially available. Heat flow from the cell shows interesting variation reflecting the characteristics of the electrode reactions. Heat generation of the cell with graphitic carbon anode draws extremely complicated curve caused by variation of stage structure of lithium intercalated graphite. The cell with hard carbon anode dissipates excess heat resulting in a voltage hysteresis between charge and discharge. In the $LiCoO_2$ cathode, thermal behaviors due to the crystal phase transition are clearly observed.

Keywords: Lithium-ion cell; Calorimetry; Graphitic carbon; Hard carbon; $LiCoO_2$

1. Introduction

Since the first commercialization of the lithium-ion cell by Sony in 1991, we have studied the thermal behavior of the cell from the viewpoint of safety [1]. In recent years, lithium-ion cells have been produced by several companies. Hallaj reported heat generation behavior depending on the discharging rate of a number of commercial cells [2]. In this study, we will describe the heat generation behaviors of various lithium-ion cells during charge and discharge with paying attention to the difference between the active electrode materials.

2. Experimental

Four kinds of commercial cells, sample A from A&T Battery, B from Panasonic, C from Sanyo, and D from Sony, were used as the test samples. All cells were cylindrical with 18 mm in diameter and 65 mm in length. The nominal electric capacity was 1500 mAh in sample A and C, 1250 mAh in B, and 1350 mAh in D.

The heat generation of the cells was measured by a twin-type heat conduction calorimeter (Setaram, C80-22) for constant current charging and discharging. Experimental setup of the calorimetry was almost same as that in our previous works [1,3], except the size of sample vessels. The test cells were charged and discharged under various conditions. A time constant of the delay due to heat transfer from the sample to the thermopile in the calorimeter was about 420–460 s depending on the sample, and the influence of the delay was corrected. The full charged state of the cells was controlled by 4.2 V constant voltage charging. Cut-off voltage of discharge was 2.7 V. The depth of discharge (DOD) of the cells was calculated from the electricity discharged actually.

3. Results and discussion

Main component materials of each sample cell were analyzed, with the result shown in Table 1. The cells were dissected into each component in an argon-filled grove-box. In the result of XRD analysis of the anode material, the XRD pattern of graphite was confirmed except D in which a weak and broad peak was observed. The manufacturer of D claims to use non-graphitizable carbon (hard carbon) as the anode active material [4]. In all samples, the XRD pattern of the cathode material was assigned to that of $LiCoO_2$. Moreover, the result of ICP analysis indicated existence of lithium and cobalt in all cathode materials. It was noteworthy that the cathode material of A was containing approximately 2 wt.% of Sn. In D, concentration ratio of lithium to cobalt was

* Corresponding author. Tel.: +81-298-61-5198; fax: +81-298-61-5805.
E-mail address: ysaito@etl.go.jp (Y. Saito).

0378-7753/01/$ – see front matter
PII: S0378-7753(01)00702-9

Table 1
Sample cells and those component materials[a]

Sample	Capacity (mAh)	Positive electrode material	Negative electrode material	Electrolyte [5]
A	1500	$LiCoO_2$ containing Sn	Graphitic carbon	EC, EMC
B	1250	$LiCoO_2$	Graphitic carbon	EC, DMC, DEC, EMC
C	1500	$LiCoO_2$	Graphitic carbon	EC, DMC, DEC
D	1350	$LiCoO_2$ (Li-rich)	Hard carbon	PC, DMC, EMC

[a] EC: ethylene carbonate; EMC: ethyl methyl carbonate; DEC: diethyl carbonate; DMC: dimethyl carbonate; PC: propylene carbonate.

extremely higher than that in the others. According to the manufacture, the cathode of D contained a little amount of Li_2CO_3, which was precursor of $LiCoO_2$ [4]. This was the origin of excess lithium in the result of ICP analysis. For the electrolyte of the sample cells, Johnson's report was referred to [5].

Fig. 1 shows examples of the results of calorimetry with the voltage profiles during charge and discharge at 313 K. The cell reaction is mostly endothermic in charge while exothermic in discharge. The main factors of the heat generation in the cells were inner resistance, electrochemical polarization, and entropy change of the cell reaction. It is possible to evaluate the entropy change at given DOD from the differentiation of the open circuit voltage (OCV) by temperature. In Fig. 1, the evaluated value of heat generation due to the entropy change at various DOD is also plotted. The shape of the heat generation curves is complicated in all samples, and it depends mainly on the entropy change.

The result of D appears unique while the others show similar variation in Fig. 1. In the voltage profile, there is a large hysteresis between charging and discharging voltage, which is a typical characteristic of the hard carbon anode [6]. Even in OCV that has been measured by intermittent charge and discharge, a hysteresis is also observed. In the heat generation curves of D, extremely large heat flow is observed at the end of discharge where is a region of (h). Only by the inner resistance, the polarization, and the entropy change, this large heat dissipation cannot be explained. In fact, even after the cut-off of the discharging current, heat continued to be generated for long time suggesting the existence of excess heat generation due to any reaction. An exothermic peak during charge at (g) in Fig. 1(D) also showed interesting behavior, whose intensity depended on the condition of the previous discharge and of the rest time just before the charge [3]. The reaction mechanism in the hard carbon anode related to the voltage hysteresis and the excess heat generation at (h) and (g) had been discussed in our past study [3]. It was suggested that in storage sites lithium was not stored electrochemically but chemically caused the hysteresis and the excess heat.

Sample A, B, and C shows step-like voltage profile that is one of typical characteristics of graphitic carbon electrode. It is well known that the lithium intercalated graphite has stage structure. The variation of voltage of Li/graphite cells depending on the stage structure was reported by Dahn [7] and Ohzuku [8]. According to Dahn's result, the stage changes in order stage-1′ (or dilute stage-1), stage-4, stage-3, liquid-like stage-2 (called stage-2L), stage-2, and stage-1, with intercalation of lithium. While a plateau is observed in the voltage profile in two-phase region of different stages, the voltage changes greatly around single stage phase region. Thus, the step-like voltage profile is drawn. Single stage phase region appears as a peak when the differentiation of voltage by charging or discharging time, dV/dt, is plotted as a function of time or DOD. In Fig. 1(A), the peaks in dV/dt were observed clearly at (b–e) with some shoulder peaks. This suggests that the anode material is attributed in single stage phase around these points. In the heat generation curve, drastic change is observed at the same regions. Fig. 2 is the result of the XRD measurement for the anode of sample A in each point including the full charged state (a) and the entirely discharged state (f). From the XRD data comparing with the Dahn's result, it is guessed that the anode is in stage-2 or stage-2L at (c) and (d), and in stage-4 at (e). Although it is difficult to distinguish stage-2 and stage-2L from the XRD data, it is suggested that (c) is in stage-2 and (d) is in stage-2L from the voltage profile and the lithium content in the anode. The anode at (b) is in two-phase region where stage-1 and stage-2 is coexistence. Hence, thermal behaviors observed around (b) is not caused by the variation of the stage structure. At the full charged state, it is also in two-phase region of stage-1 and stage-2, however, the XRD peak of stage-2 is shifted to lower angle. At the entirely discharged state, the anode is in stage-1′. It is concluded that the complicated variation of the heat generation curve is observed due to the change of the stage structure of lithium intercalated graphite during charge and discharge in lithium-ion cells with graphitic carbon anode. Fine distinction of the variation among sample A, B and C seems to originate in the characteristics such as crystallinity and size of the crystallite of the anode material. The calorimetry is useful method to analyze the variation of stage structure of the lithium intercalated graphite.

In all samples, peak behaviors are observed around (b) in the heat generation curve. As mentioned above, these peaks are not caused by the change of stage structure in the graphitic carbon anode. In addition, it is observed in D in which hard carbon is used as the anode active material.

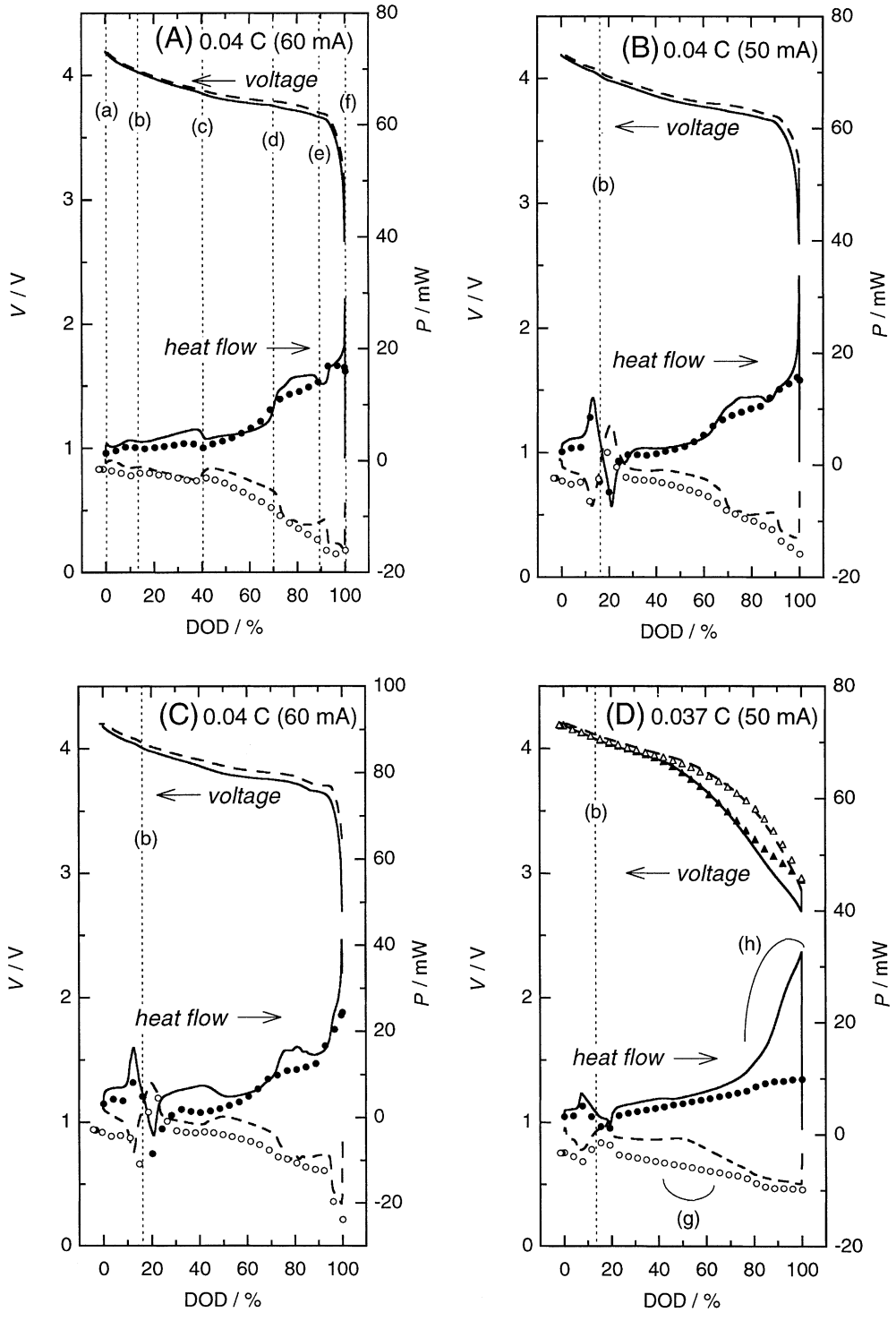

Fig. 1. Terminal voltage of the sample cell (V) and heat flow from the cell (P) during constant current charge (dashed line) and discharge (solid line) at 313 K. A, B, C, and D indicate sample names. Open and closed circles are heat generation due to entropy change of the cell reaction during charge and discharge, respectively. Open and closed triangles in D are open circuit voltage measured by intermittent charge and discharge, respectively.

Hence, these peaks are thought to originate in the cathode active materials. In fact, it had been already suggested from our calorimetric study in which the temperature dependence of the peak behavior had been investigated [1]. The crystal structure of the cathode active material Li_xCoO_2 is usually hexagonal at room temperature, while it changes to monoclinic in the small composition range around $x = 0.5$ [9]. Actually, XRD pattern assigned as monoclinic is obtained from the cathode material of all cells at (b) in DOD. Thus, the thermal peaks around (b) were found to be caused by the

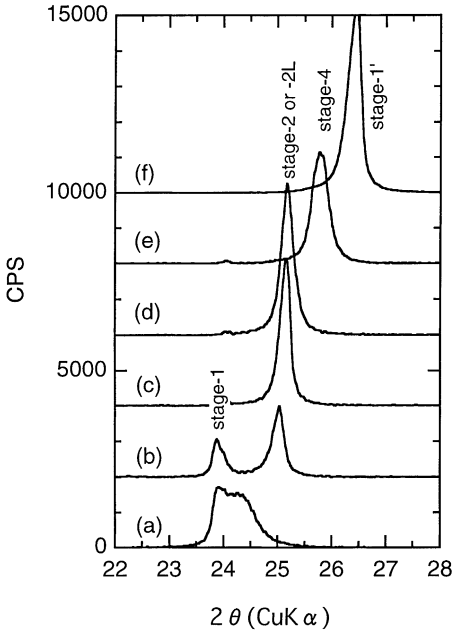

Fig. 2. XRD spectra for anode material of sample A. For DOD of the sample refer Fig. 1(A).

crystal phase transition of the cathode material. The calorimetric results indicate that the phase transition from hexagonal to monoclinic is exothermic, and the reverse transition is endothermic, that agree with the results of Hong's calorimetric work for lithium-ion cells [10].

Fig. 3 shows DSC curves of the cathode material at (b). The samples has been rinsed in ethyl methyl carbonate and dried in an evacuated flask at 340 K before the DSC measurement in order to reduce the influence of the electrolyte. In Fig. 3, a large endothermic peak can be seen in all samples, of which onset temperature is 278, 326, 320 and 285 K in A, B, C and D, respectively. In addition, a small endothermic sub-peak is observed at 290 K in B and at 325 K in D. In sample A, the main peak has shoulders, however, they disappear in the second scan. XRD measurement at various temperatures between 223 and 373 K was also carried out for the cathode materials at (b). As the result, the main DSC peak in all cells was found to originate in the crystal phase transition from monoclinic to hexagonal structures. Any remarkable structure changes were not observed in the XRD data corresponding to the sub-peaks in B and D. In Reimers' report on Li_xCoO_2 [9], the transition temperature (T_e) between monoclinic and hexagonal is about 330 K when x is 0.5, where the plot of dx/dVversus x has a minimum. Since DOD of (b) is decided from a maximum peak in dV/dt, it can be concluded that T_e in B and C agrees with that in Reimers' result. On the other hand, T_e is shifted to lower temperature in A and D. This is the reason why the intensity of thermal peaks around (b) in Fig. 1 is small in A and D. Actually, even in A and D, clearer and larger peaks were observed around (b) in the calorimetry in charge and discharge at lower temperature. As mentioned above, the cathode active material of A contains Sn, and this might be the cause of the lower T_e. Similarly in D, since the cathode is rich in lithium, excess lithium might form defect structure in the crystal of $LiCoO_2$ resulting in depression of T_e. It is also suggested that the small DSC peak observed at 325 K in D originates in the cathode particles without the defect and that the peak in B at 290 K is derived from any defect structure. These results suggest that introduction of defect structure into $LiCoO_2$ is effective to suppress the phase transition.

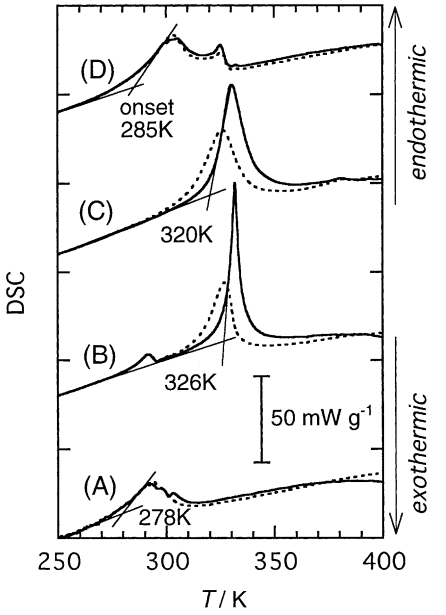

Fig. 3. DSC curves of cathode material. A, B, C, and D indicate sample names. DOD of each sample is controlled to that shown in Fig. 1(b). The scanning rate is 10 K min^{-1}. Solid and dashed lines are the results of first and second scans, respectively.

4. Conclusions

Calorimetry during charge and discharge was carried out for various lithium-ion cells. If the graphitic carbon material was used in the cell as the anode, complicated thermal behaviors caused by variation of the stage structure were observed. In the case of the hard carbon anode, excess heat generation was observed which related to hysteresis of the voltage profile. Thermal behaviors originated from the crystal phase transition of the cathode active material, Li_xCoO_2, were also detected. The transition was endothermic in the direction from monoclinic to hexagonal structures. Although all test cells had L_xCoO_2-based cathode material, the transition temperature depended on the cells.

References

[1] Y. Saito, K. Kanari, K. Takano, J. Power Sources 68 (1997) 451.
[2] S.A. Hallaj, J. Prakash, J.R. Selman, J. Power Sources 87 (2000) 186.

[3] Y. Saito, K. Takano, K. Kanari, K. Nozaki, Mater. Res. Soc. Symp. Proc. 496 (1998) 551.
[4] K. Ozawa, Solid State Ionics 69 (1994) 212.
[5] B.A. Johnson, R.E. White, J. Power Sources 70 (1998) 48.
[6] J.R. Dahn, T. Zheng, Y. Liu, J.S. Xue, Science 270 (1995) 590.
[7] J.R. Dahn, Phys. Rev. B 44 (1991) 9170.
[8] T. Ohzuku, Y. Iwakoshi, K. Sawai, J. Electrochem. Soc. 140 (1993) 2490.
[9] J.N. Reimers, J.R. Dahn, J. Electrochem. Soc. 139 (1992) 2091.
[10] J.-S. Hong, J.R. Selman, J. Electrochem. Soc. 147 (2000) 3183.